ORIGINAL PAPER

Alkali-modified biochar as a sustainable adsorbent for the low-temperature uptake of nitric oxide

S. I. Anthonysamy[1] · P. Lahijani[2] · M. Mohammadi[3] · A. R. Mohamed[1]

Abstract

Nitric oxide (NO) as the major constituent of nitrogen oxides (NO_x), which is mainly emitted from combustion processes, is responsible for several environmental and health issues, and the control of its emission is a global concern. In this regard, this study investigates low-temperature oxidative uptake of NO on alkali-modified biochar. Rubber seed shell was utilized as a locally available lignocellulosic waste to develop biochar through slow pyrolysis. The porosity attributes and surface chemistry of the developed biochar were then improved through alkali modification. The NO capture capacity of KOH, NaOH, K_2CO_3 and Na_2CO_3-activated biochars was 63.0, 59.3, 59.0 and 58.5 mg/g, respectively, which was considerably higher than that of the pristine biochar, 17.8 mg/g. This considerable improvement was mainly attributed to the introduction of more oxygen functionalities, improvement of microporosity and creation of more carbon defects in the biochar, after alkali modification. With some investigations on the alkali agent/biochar impregnation ratio, the adsorption capacity of the KOH-activated biochar (at a ratio of 2:1 (w/w)) could be improved to 87.0 mg/g at 30 °C. Characterization studies using FTIR and XPS suggested that the adsorbed species on the biochar surface was in the form of monodentate nitrito (–O–N=O), which was formed from the oxidation of NO on the surface-oxidized groups. Kinetic studies using pseudo-first, pseudo-second and Elovich models indicated that the adsorption of NO on KOH-activated biochar surface was mainly controlled by a physisorption or a weak chemisorption process, with a low activation energy of − 29 kJ/mol.

Keywords Biochar · Elovich model · Nitric oxide uptake · Rubber seed shell · Surface chemistry

Introduction

The presence of nitrogen oxides (NO_x) in various forms, including nitric oxide (NO) and nitrogen dioxide (NO_2), in industrial flue gases is a major environmental problem. These toxic gases are responsible for several environmental issues including acid rain, photochemical smog and ozone layer depletion, besides causing serious respiratory diseases

in human (Shen et al. 2016; Yang et al. 2019). Despite the development of new materials and emerging processes for the control of environmental pollution, NO_x emissions have remained a global concern (Deng et al. 2020). Among the technologies developed for the control of NO_x emission is the selective catalytic reduction (SCR) using ammonia (NH_3) which has been implemented since its first industrial application in the 1970s in Japan (You et al. 2017). Nevertheless, the process has several drawbacks including high reaction temperature (> 300 °C), ammonia leakage, un-reacted reducing agent and extra expenses to replace deactivated catalysts (Shen et al. 2016; You et al. 2017). Hence, the development of a cost-effective and greener NO_x abatement technology at ambient temperature is highly demanded.

Since a majority of fossil fuel-derived NO_x is in the form of NO (around 90%) (Al-Rahbi and Williams 2016) and considering the stability of NO in the ambient air, which can hardly react with O_2 or be absorbed by water (You et al. 2019), catalytic oxidation of NO to NO_2 at ambient temperature and then condensation of NO_2 in the pores of adsorbent

✉ A. R. Mohamed
  chrahman@usm.my

1   Low Carbon Economy (LCE) Research Group, School of Chemical Engineering, Universiti Sains Malaysia, 14300 Nibong Tebal, Pulau Pinang, Malaysia

2   School of Aerospace Engineering, Universiti Sains Malaysia, 14300 Nibong Tebal, Pulau Pinang, Malaysia

3   Faculty of Chemical Engineering, Babol Noshirvani University of Technology, 47148 Babol, Iran

can be a promising route to control the emission of NO. Since the van der Waals constant (a) for NO_2 is nearly four times higher than that for NO (Rubel and Stencel 1996), its physical adsorption on solid sorbents is much higher than NO. Hence, it is reasonable to first oxidize NO to NO_2 and then adsorb it. Subsequently, the adsorbed NO_2, which is up to 254 times more soluble than NO (Ghafari and Atkinson 2016), can be removed as nitric acid using water or basic solutions, with around 100% efficiency (Deng et al. 2020). Even the inclusion of NO oxidation step before the SCR process can enhance the SCR reaction rate (Shen et al. 2016). Therefore, NO oxidation can be utilized either as a standalone process or in combination with the existing SCR technology for NO_x emission abatement.

So far, some attempts have been made for catalytic oxidation of NO over carbon-based materials. Some examples are the use of pristine or chemically modified activated carbon (Zhang et al. 2008; Al-Rahbi and Williams 2016; Ghafari and Atkinson 2016; Yang et al. 2018), nitric acid hydrothermally treated activated carbon (You et al. 2019), manganese oxide (MnO_x)-loaded activated carbon (You et al. 2017), sewage sludge-derived char (Deng et al. 2020), activated carbon fiber (Adapa et al. 2006) and ordered mesoporous carbon (Cao et al. 2014; Chen et al. 2014) for NO adsorption. However, there is an ongoing research to develop efficient carbon-based adsorbents from low-cost and sustainable materials. Thanks to the abundance and low price of agro-wastes and agricultural residues, carbon-based sorbents can be produced cost-effectively at large scales for several applications. Biochar, which is the carbonaceous solid product obtained through thermal conversion (pyrolysis, torrefaction, hydrothermal carbonization and gasification) of biomass (Gargiulo et al. 2018), has recently attracted special attention. It has potential applications in the fields of agriculture (as soil fertilizer), climate change (as carbon capture and storage material) and environmental remediation (adsorption of pollutants and wastewater treatment) (Xiao et al. 2018). Compared to the activated carbon whose application for gas- and liquid-phase adsorption has been numerously reported (Nayl et al. 2017; Abdulrasheed et al. 2018; Bakar et al. 2021; Jjagwe et al. 2021), adsorption using biochar is an emerging field of study and there is an ongoing research on various aspects of its production and application. Advantageously, the conducted studies on activated carbon would provide an immense source of information for biochar research.

Recently, metal oxide-loaded biochar has been used for SCR of NO with NH_3 at low temperature (Kong et al. 2018; Yang et al. 2019); nevertheless, reports on the use of biochar for catalytic oxidation of NO are still very scarce (Anthonysamy et al. 2020). Carbon defects and dangling bonds at the edge of char can serve as active sites for the conversion of NO to NO_2 in the presence of oxygen (Guo et al. 2015). Moreover,

the oxygenated functional groups (such as hydroxyl, carboxyl, and carbonyl), which are responsible for a rich and complex surface chemistry of biochar, can significantly contribute to the oxidation reaction. Advantageously, the surface chemistry of biochar can be modulated through physical/chemical/physicochemical modifications (Xiao et al. 2018) to introduce more surface oxygen functional groups, which are known to be beneficial for NO adsorption and/or NO oxidation to NO_2 (Adapa et al. 2006).

Malaysia is the third largest producer of natural rubber after Thailand and Indonesia (Reshad et al. 2018). Latex as source of natural rubber is harvested from the rubber tree (*Hevea brasiliensis*), which is widely cultivated in Malaysia. The tree has a by-product, rubber seed, which has an oil-rich kernel. During the oil extraction process, significant amounts of rubber seed shell (RSS) are produced that pose waste disposal problems to rubber seed oil millers (Lahijani et al. 2019). Due to the abundance and low cost of this lignocellulosic waste in Malaysia, production of biochar from RSS would be a sustainable, economic, and environmentally friendly approach for the conversion of waste into value-added product. Moreover, production of biomass-based adsorbent with high NO_x uptake at low temperature would enhance the practical feasibility of the NO_x abatement systems. Advantageously, the development of biochar from RSS and its utilization as a catalytic carbon material for NO oxidation and uptake would be a viable solution to address two environmental issues: (i) waste disposal problems in rubber seed oil mill plants through the conversion of biomass residues to value-added product and (ii) control of NO_x emission from combustion sources using the RSS-derived biochar as adsorbent for NO uptake. In this context, the current study investigated the development of RSS-derived alkali-activated biochar for NO adsorption. To the best of authors' knowledge, studies on the use of pristine/modified biochar for NO uptake are very scarce, and this study is among the first reports on the use of modified biochar for NO oxidation and uptake. The influence of different alkali materials, activation temperature, and alkali material/biochar impregnation ratio on NO uptake capacity was investigated, and the results were discussed with the help of several characterization techniques. The kinetics of the adsorption process was also studied, and the possible governing mechanism of the reaction was verified. This study was conducted at the School of Chemical Engineering, Universiti Sains Malaysia (USM), from February to October 2020.

Materials and methods

Biomass feedstock

Rubber seed shell (RSS) was used as the lignocellulosic feedstock to prepare biochar. The shells were collected from

a rubber tree plantation area in Serdang, Perak, Malaysia. The shells were washed, oven-dried and then crushed using a mechanical crusher to a particle size of around 150 μm. Proximate analysis was carried out on the RSS biomass using a thermogravimetric analyzer (TGA, SDTQ-600). Accordingly, the RSS contained 77.7% moisture, 0.4% ash and 21.9% fixed carbon on a dry weight basis. Ultimate analysis was carried out using a PerkinElmer 2400 Series II CHNS/O elemental analyzer. According to the results, the RSS biomass consisted of 48.36% carbon, 45.45% oxygen, 5.75% hydrogen, 0.30% sulfur and 0.14% nitrogen, on a dry basis.

Preparation of alkali-loaded biochar

RSS biochar was developed through slow pyrolysis of biomass at 700 °C for 90 min. The obtained biochar was ground and sieved to a particle size of 63 μm. To modify the surface properties of biochar, post-synthesis procedure was used where the RSS biochar was impregnated with several alkali agents including potassium hydroxide (KOH), potassium carbonate (K_2CO_3), sodium hydroxide (NaOH) and sodium carbonate (Na_2CO_3) at a mass ratio of 3:1 (alkali chemical/biochar). The effect of selected alkali concentration was then studied by changing the alkali chemical/biochar mass ratio from 1:1 to 3:1. The chemically activated biochar was then heated under N_2 at different temperatures (600, 700, 800 and 900 °C) for 3 h. Afterward, the biochar sample was cooled down under the same atmosphere; then, it was washed with HCl and distilled water until a neutral pH was reached in washing water. Finally, the samples were oven-dried at 105 °C and stored in airtight containers for adsorption experiments.

NO adsorption study

The NO adsorption studies were carried out under isothermal condition in a thermogravimetric analyzer (TGA, SDTQ-600), with ± 1 μg accuracy. In a typical adsorption experiment, about 8 mg of biochar was loaded in a pan and heated under N_2 to 120 °C for 20 min. This was for desorption of any moisture or gas molecules, which might be pre-adsorbed by the biochar. In the next step, the sample was cooled down under N_2 to the preset adsorption temperature (30, 40, 50 and 70 °C). Once the desired temperature was reached, a mixed gas containing 2000 ppm NO in N_2 was flowed over the sample for 180 min. During the adsorption process, the weight gain of biochar was continuously recorded for calculation of the NO adsorption capacity as mg NO/g of adsorbent. Control adsorption tests were conducted for each sample using pure N_2 gas; this was to ensure that the observed weight gain was associated with the NO

adsorption, not N_2 capture. To assure the repeatability of the results, adsorption tests were replicated twice.

Characterization

To analyze the surface functional groups of RSS-derived biochar samples, a Thermo Scientific Nicolet iS10 Fourier transform infrared (FTIR) spectrometer was used. The surface morphology of the biochar was studied using a Quanta 450 FEG scanning electron microscope (SEM). The intrinsic carbon structure of the developed biochar samples was analyzed using a Renishaw's inVia Raman spectrometer. To analyze the carbon structure of the developed biochar and mineralogical analysis, X-ray diffraction (XRD) spectra were recorded on a *X' Pert* Pro diffractometer with Cu target Kα-ray. To determine the surface area and porosity characteristics of the prepared biochar samples, a Micromeritics ASAP 2010 volumetric apparatus was used to carry out the N_2 adsorption tests. The chemical state and concentration of elements on the biochar surface were determined through X-ray photoelectron spectroscopy (XPS) analysis carried out using a ULVAC-PHI QuantERA II XPS equipped with an Al Kα X-ray source ($hv = 1486.6$ eV). The surface basic oxides of selected samples were determined using the Boehm titration method (Ahmad et al. 2013).

Results and discussion

Effect of alkali activation

Biochar was developed from slow pyrolysis of RSS biomass at 700 °C for 90 min with a yield of 13.7%, yet the porosity properties of the prepared biochar were poor. Thus, some sort of modifications was needed to improve the porosity attributes and surface chemistry of the parent biochar before it could be exploited for NO adsorption. According to the study of Nowicki et al. (2010), activation of carbon samples through chemical routes introduced much greater content of oxygen groups on the surface compared to the physical method. Additionally, alkaline activation of biochar has been reported to increase the oxygen content and surface basicity (Li et al. 2020). Therefore, in this study, post-synthesis activation using alkali chemicals including KOH, NaOH, K_2CO_3 and Na_2CO_3 was used to address the poor porosity characteristics of biochar and improve its surface chemistry. All chemically activated biochar samples were subjected to NO adsorption (0.2% NO in N_2) at 30 °C, and their adsorption capacity was compared to that of pristine biochar. Figure 1 demonstrates the NO adsorption capacity of different alkali-impregnated biochar samples compared to the pristine RSS biochar. All alkali-modified biochars revealed almost overlapped trends in NO adsorption with comparable adsorption

capacities, yet their adsorption capacity was considerably higher than that of parent biochar. The obtained adsorption capacities were 63.0, 59.3, 59.0 and 58.5 mg/g for KOH, NaOH, K_2CO_3 and Na_2CO_3 activated biochars, respectively, while the sorption capacity of the pristine biochar was only 17.8 mg/g. Similar adsorption tests were carried out using pure N_2 (referred to as control) to assure that the observed adsorption capacities were associated with NO adsorption, not N_2. The amount of N_2 adsorbed by all biochar samples was quite low, around 3.0 mg/g for pristine biochar and less than 6.8 mg/g for chemically activated biochars (Fig. S1, Supplementary Material). The kinetic diameters of N_2, NO and NO_2, which are 0.364, 0.317 and 0.340 nm, respectively, differ only slightly; hence, any pore filling because of steric effects would be insignificant. Micropore filling is known to be only effective for gases with the critical temperatures (T_C) higher than the adsorption temperature (Rubel and Stencel 1996). Accordingly, at the adsorption temperature range of this study (303 to 343 K), the adsorption of N_2 and NO with T_C values of 126 and 180 K, respectively, in micropores was insignificant, while NO_2 with T_C of 431 K had a high potential to be adsorbed in micropores. Additionally, the extent of micropore filling is known to be in relation to the van der Waals constant a in carbon materials, and since this constant for NO_2 is almost four times that of NO, thus NO_2 has a higher potential to be adsorbed in micropores (Rubel and Stencel 1996). Hence, NO is probably captured from the gas stream and condensed as NO_2 within the micropores of biochar.

Comparison of the NO uptake capacity of chemically activated and pristine biochars (Fig. 1) indicates that alkali activation of biochar was a successful approach to significantly enhance the NO adsorption capacity. In fact, the use of these bases was to: (i) modify the porous structure of biochar, (ii) introduc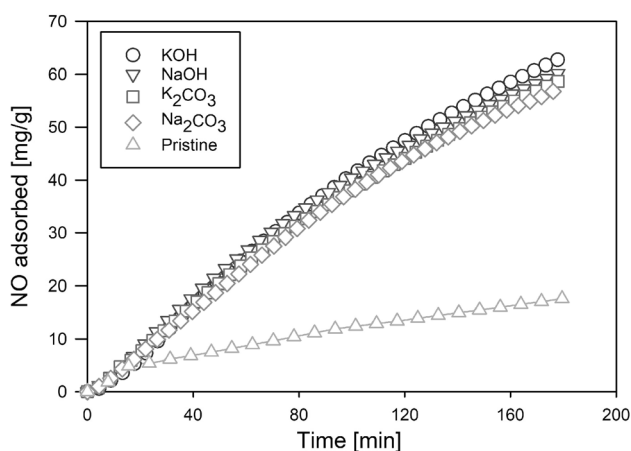e more oxygen-containing functional groups on the biochar surface and (iii) improve the surface basicity of biochar. Alkali metals including K and Na are known as excellent catalysts for catalyzing the char gasification reaction (Lahijani et al. 2015). Indeed, the reaction of carbon with *in situ*-produced CO_2 at high temperature (char gasification: $C + CO_2 \leftrightarrow 2CO$) in the presence of such catalysts leads to the development of pore structure and enlargement of the surface area. Use of these base chemicals could also increase the surface alkalinity, which is much beneficial for the adsorption of NO gas with acidic character. Moreover, the surface oxidation of NO to NO_2 becomes possible in the presence of oxygen; hence, the use of these chemicals to increase the oxygen content on biochar surface could enhance the adsorption and/or oxidation of NO. Therefore, these effects could cooperatively enhance the NO adsorption capacity of biochar after alkali modification, and the results in Fig. 1 evidently show such synergy among these factors, which collectively influenced the adsorption performance; the adsorption capacity of alkali-activated biochars was almost 3.3 to 3.5 times that of virgin biochar.

Figure 2a shows the XRD patterns of pristine as well as alkali-modified RSS biochars. Two broad peaks were observed at 2θ around 15° and 23° in all patterns, corresponding to C(002) diffraction peaks, which indicate an amorphous carbon structure with randomly oriented aromatic carbon sheets (Yu et al. 2011). Some sharp peaks also appeared in the pattern of the pristine biochar at $2\theta = 20°$, 22° and 26°, which could be associated with the inorganic compounds in biochar ash (Dehkhoda et al. 2014); nevertheless, these peaks almost eliminated or significantly reduced after modification with alkali chemicals signifying the removal of the majority of these compounds. No specific peaks corresponding to the used alkali chemicals were observed in the XRD patterns of alkali-modified biochars, probably because of the decomposition of these compounds during the activation step. The highly amorphous feature of biochar could be another reason for not observing any obvious crystalline diffraction peaks associated with the alkali chemicals (Yang et al. 2018).

To further study the carbon structure of the developed biochars, Raman analysis was carried out and the results are presented in Fig. 2b. Two main peaks can be observed in the range of 1330 to 1356 cm^{-1} and 1590 to 1606 cm^{-1} corresponding to the *D*- and *G*-bands, respectively. The *D*-band indicates the amorphous carbon structure, including defects and disordered carbon, while the *G*-band represents the crystalline phase of carbon in biochar. The intensity ratio I_D/I_G can be indicative of the graphitization degree of carbon where the smaller this ratio, the higher is the graphitic degree. A comparison of the Raman spectrum of the pristine biochar with those of alkali-modified biochars indicates the noticeable effect of alkali impregnation on the development of amorphous phase in biochar where the I_D/I_G increased from 0.86 in the parent biochar
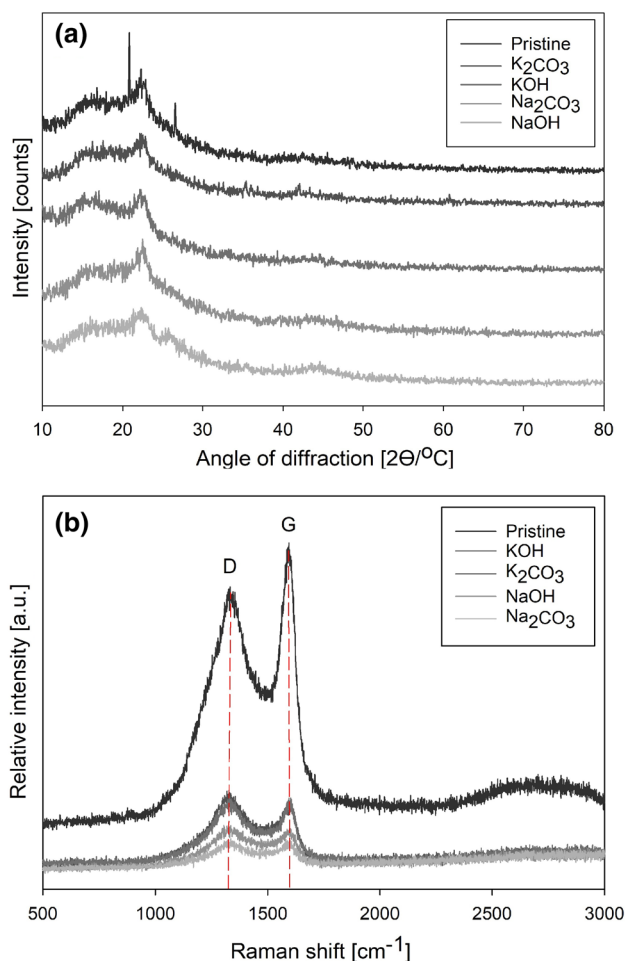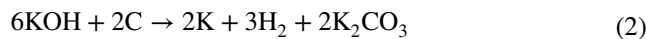

Fig. 1 NO uptake capacity of pristine and alkali-activated RSS biochars at 30 °C

Fig. 2 a XRD patterns of pristine and alkali-activated RSS biochars and **b** Raman spectra of pristine and alkali-activated RSS biochars

to 0.99, 1.00, 1.05 and 1.10 in K_2CO_3-, Na_2CO_3-, NaOH- and KOH-activated biochars, respectively. Such breakdown of carbon symmetry and creation of disordered carbon after alkali activation significantly promoted the NO adsorption capacity of the modified biochars (Fig. 1). This was mainly attributed to the formation of more carbon defects after alkali activation, which act as active sites for the adsorption of NO and/or its oxidation to NO_2 in the presence of oxygen (Guo et al. 2015). Among the modified biochars, KOH-activated biochar showed the lowest degree of graphitization, which is consistent with the highest NO sorption capacity attained using this adsorbent. Hence, the following NO adsorption studies were carried out on KOH-activated biochar only.

The mechanism of activation of biochar using KOH follows the reactions represented in Eqs. (1) to (3) at temperatures above 600 °C (Ding and Liu 2020):

$$2KOH \leftrightarrow K_2O + H_2O \tag{1}$$

$$6KOH + 2C \rightarrow 2K + 3H_2 + 2K_2CO_3 \tag{2}$$

$$K_2CO_3 \leftrightarrow K_2O + CO_2. \tag{3}$$

The formed potassium species, i.e., K_2CO_3 and K_2O, could diffuse into the structure of biochar and cause the expansion of existing pores and/or creation of new ones (Li et al. 2020). The reaction of K_2CO_3 with char also increases the creation of complex salts (C–O–K) at the carbon surface (Dıaz-Terán et al. 2003). As the activation temperature increases to beyond 650 °C, the produced K_2CO_3 and K_2O species might be substantially reduced by carbon to produce metallic K according to Eqs. (4) and (5) (Dıaz-Terán et al. 2003):

$$K_2CO_3 + 2C \rightarrow 2K + 3CO \tag{4}$$

$$K_2O + C \rightarrow 2K + CO. \tag{5}$$

The consumption of carbon through these reactions significantly contributes to porosity development, which is much desired to obtain a porous adsorbent. The intercalation of potassium vapor (K^+ ion) within crystallites of condensed carbon expands the interlayer distancing of graphitic layers of biochar and etching of carbon atoms with K^+ leads to the creation of micropores and/or small mesopores (Yang et al. 2018). Moreover, the *in situ*-produced CO_2 from the decomposition of K_2CO_3 (Eq. 3) can react with carbon following the Boudouard reaction, also known as char gasification, whose occurrence is closely associated with pore structure development (Lahijani et al. 2015):

$$CO_2 + C \rightarrow 2CO. \tag{6}$$

Hence, KOH activation is an efficient method to develop highly microporous carbon with high surface oxygen complexes due to the intercalation of K into the graphitic layers of carbon, oxidation of carbon and its activation by in situ-produced CO_2 (Nowicki et al. 2010).

Effect of activation temperature

The effect of activation temperature on the NO uptake capacity of KOH-activated biochar is shown in Fig. 3a. The NO adsorption capacity of the KOH-impregnated biochar, activated at 600 °C, was 43.8 mg/g; with further increase of the activation temperature to 700, 800 and 900 °C, the capture capacity remained around 63.0 mg/g. As discussed by many researchers, activation temperature has a critical effect on the type and amount of surface oxides (Nowicki et al. 2010; Belhachemi et al. 2014). Due to the acidic character of NO, the presence of basic groups on the adsorbent surface is beneficial for the adsorption of this gas. The concentration of basic groups on the KOH-impregnated biochar
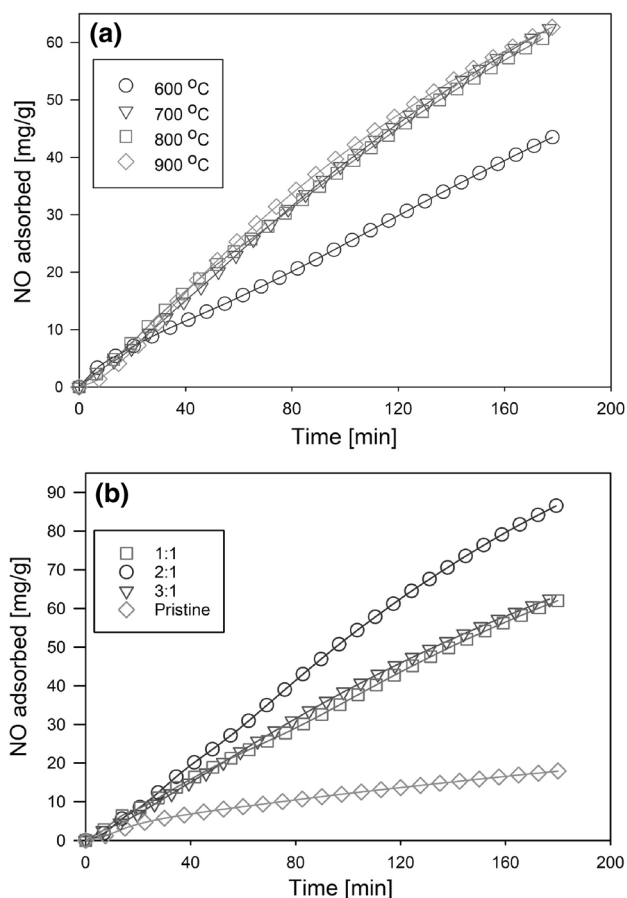
Fig. 3 NO uptake capacity of KOH-impregnated biochars at different **a** activation temperatures and **b** impregnation ratios (KOH/biochar)

Table 1 Surface area and porosity properties of KOH-activated biochars at different impregnation ratios

KOH: biochar (w/w)	S_{BET} (m²/g)	V_t (cm³/g)	V_{mic} (cm³/g)	Average pore size (Å)
1:1	391.48	0.214	0.159	30.69
2:1	377.87	0.196	0.158	34.16
3:1	712.10	0.360	0.291	28.48

the consideration. Since increase of the activation temperature to beyond 700 °C was not beneficial for enhancing the NO uptake capacity, in the subsequent experiments all the samples were activated at 700 °C for 3 h.

Effect of KOH impregnation ratio

The effect of KOH/biochar impregnation ratio on the NO adsorption capacity was studied by varying this ratio in the range of 1:1 to 3:1. Figure 3b depicts the NO capture capacity of the resulting KOH-activated biochars. Increase of the ratio from 1:1 to 2:1 considerably enhanced the NO adsorption capacity from 62.0 to 87.0 mg/g, yet with further increase of the impregnation ratio to 3:1, the adsorption capacity dropped to 63.0 mg/g. It is well known that besides surface chemical influences, physical properties of the adsorbent are also important for the uptake of the adsorbate. For this, surface area and porosity properties of the KOH-activated biochars were analyzed, and the results are shown in Fig. S2 (Supplementary Material) and Table 1. The N_2 adsorption–desorption isotherms for all samples were type I(b), according to the IUPAC classification, which are found in materials with a broad range of pore size, including wide micropores and possibly narrow mesopores (below 2.5 nm) (Thommes et al. 2015). The KOH-impregnated biochar samples at ratios 1:1 and 2:1 represented a relatively broad H4-type hysteresis loop, which often occurs in micro-mesoporous carbons and indicates the presence of narrow slit-shape pores (Thommes et al. 2015). Interestingly, the SEM image of KOH-impregnated (2:1) biochar also revealed the presence of slit-like pores on the biochar surface (Fig. S3, Supplementary Material).

Comparison of the NO uptake capacity of the samples with respect to their porosity properties (Table 1) indicated there were no correlations between the BET surface areas and the NO adsorption capacities. Therefore, other chemical or physical factors might had influenced the uptake capacity of the biochars. The absence of correlation between the BET surface area and uptake capacity was also reported by Rubel et al. (1995), and they concluded that pore structure/size distribution was an important factor affecting the selective NO capture capacity. Adapa et al. (2006) also discussed that the BET surface area and micropore volume were not

activated at 600, 700, 800 and 900 °C, as determined by Boehm titration method, was 4.6, 6.3, 7.9 and 9.0 mmol/g, respectively. Increase of the activation temperature to above 600 °C considerably increased the number of basic groups. Nowicki et al. (2010) also reported that the sample activated using KOH at 500 °C contained the lowest amount of basic groups and the highest concentration of acidic group, and increase of the activation temperature to 800 °C increased the number of basic groups by 2–3 times. The rise in the surface basicity with increase of the activation temperature was attributed to the removal of strong basic groups such as carboxyl, lactones and anhydrides at lower temperatures and other acidic functional groups like phenols and carbonyls at higher temperatures (Belhachemi et al. 2014). Accordingly, the use of higher activation temperatures favored the generation of more basic groups. Although the increase of the activation temperature from 700 to 900 °C increased the number of basic groups, the NO adsorption capacity remained unchanged. Thus, it may be inferred that surface basicity is not the sole factor, which affects the NO adsorption, and the contribution of other factors such as porosity and carbon defects to NO uptake should also be taken into

the primary factors influencing the oxidation of NO on the surface of activated carbon fiber, but the effect of surface oxygen groups was predominant. Zhang et al. (2008) also observed that the oxidation of NO to NO_2 over activated carbon was independent of the surface area. According to the porosity characteristics of the developed KOH-activated biochars, the sample impregnated at a ratio of 2:1 with slightly larger pore size (3.4 nm) showed the highest NO uptake capacity of 87.0 mg/g. Although micropores have a very high potential for gas adsorption, the adsorption capacity in micropores is low because only a single layer of gas molecules can be adsorbed (Alcañiz-Monge et al. 2008), while in mesopores the adsorption potential is low, yet the mass transfer and internal surface diffusion limitations are less, permitting easier entrance of NO molecules into the pore structure of biochar (Alcañiz-Monge et al. 2008; Chen et al. 2014). Therefore, the higher uptake capacity of the biochar impregnated with KOH at a ratio of 2:1 compared to the other samples should be attributed to its larger pore size and the contribution of mesopores, as inferred from the appeared hysteresis loop, to the adsorption process. In fact, when micropores are filled with the adsorbed species only mesopore surface area would be available for the reaction (Shen et al. 2016). Such contribution of mesopores of activated carbon to the NO uptake was also reported by Chen et al. 2014.

Adsorption mechanism

Many studies have discussed besides physical properties and surface chemistry of the adsorbent; in particular, surface–oxygen complexes influence the selective NO uptake (Rubel et al. 1995; Adapa et al. 2006; Shen et al. 2016). If NO is to coordinate as a Lewis acid with surface oxygen to form NO_2, then the presence and nature of surface oxygen complexes are of utmost importance. In fact, the carbon surface oxides are considered as the active sites that initiate the reactions with NO in gas phase (Rubel et al. 1995). To gain some insights into the surface oxygen functionalities and to clarify the possible mechanism for NO adsorption on biochar, the surface chemical properties of the fresh (before adsorption) and spent (after adsorption) biochars (pristine and KOH-activated biochar (2:1)) were analyzed by FTIR and XPS analyses. Figure 4 exhibits the FTIR spectra of the pristine and KOH-activated biochars, before and after NO adsorption. The distinctive peaks in all spectra are the one around 3400 cm^{-1} (O–H stretching vibration), the peaks near 1560 and 1620 cm^{-1} (C=C or C=O stretching in aromatic ring) (Cheng et al. 2020) and a wide peak around 1080 cm^{-1} (C–O stretching vibration) (Li et al. 2016; You et al. 2019). Comparison of the spectra of pristine and KOH-activated biochars signifies the intensity of the peak located around 1080 cm^{-1} became remarkably stronger after KOH
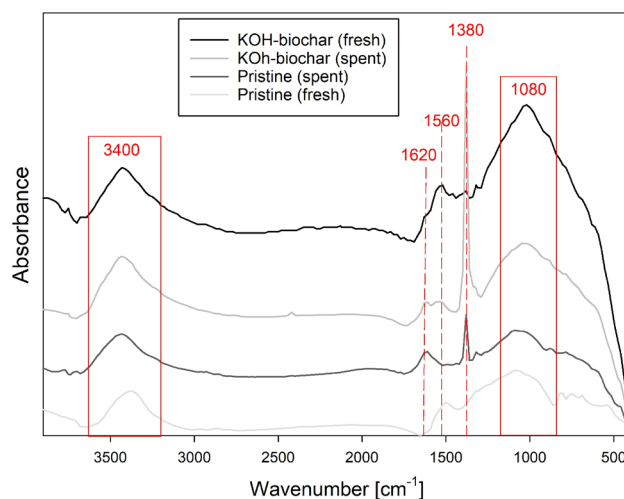

Fig. 4 FTIR spectra of pristine and KOH-activated biochar (2:1) before and after NO adsorption at 30 °C

activation. This was confidently attributed to the oxidation and activation effect of KOH, which introduced more oxygen-containing functional groups on biochar surface. Furthermore, a comparison of the FTIR spectra of fresh and spent biochars indicates the presence of a very sharp peak around 1380 cm^{-1} in the spectra of spent adsorbents whose intensity is much stronger for the spent KOH-activated biochar. This band should be associated with the formation of a new species on biochar surface after NO adsorption. According to Cao et al. (2014), this peak could be assigned to the stretching vibration of N−O and N=O bands in –O–N=O. It is most probable that the NO molecule was adsorbed on the biochar surface in the form of C–O–N=O. The considerably higher intensity of this peak in the spectrum of spent KOH-activated biochar in comparison with that of spent pristine biochar is consistent with the remarkably higher sorption capacity of activated biochar (87.0 mg/g) compared to that of pristine biochar (17.8 mg/g). With the emergence of this peak after NO adsorption, it can be assumed that NO is first oxidized to NO_2 in the presence of surface oxygen groups and then adsorbed in the pores. To further confirm such premise, XPS analysis was carried out on the biochar sample before and after NO adsorption.

Figure 5 shows the curve fitting of O 1s spectrum for the fresh KOH-activated biochar that was deconvoluted into four peaks. The peak with binding energy of 530.51 eV (O1) corresponds to the aromatic C=O (Herath et al. 2020), the one located around 531.21 eV (O2) is attributed to the K–O bond (Dıaz-Terán et al. 2003), the peak with binding energy of 532.24 eV (O3) represents the C–O bond in aromatic rings or in ethers and phenols (Lee et al. 2002) and the peak around 533.50 eV (O4) is assigned to the O–C=O bond in carboxyl groups (Ding and Liu 2020). The same deconvoluted peaks at binding energies of 530.52, 531.63,
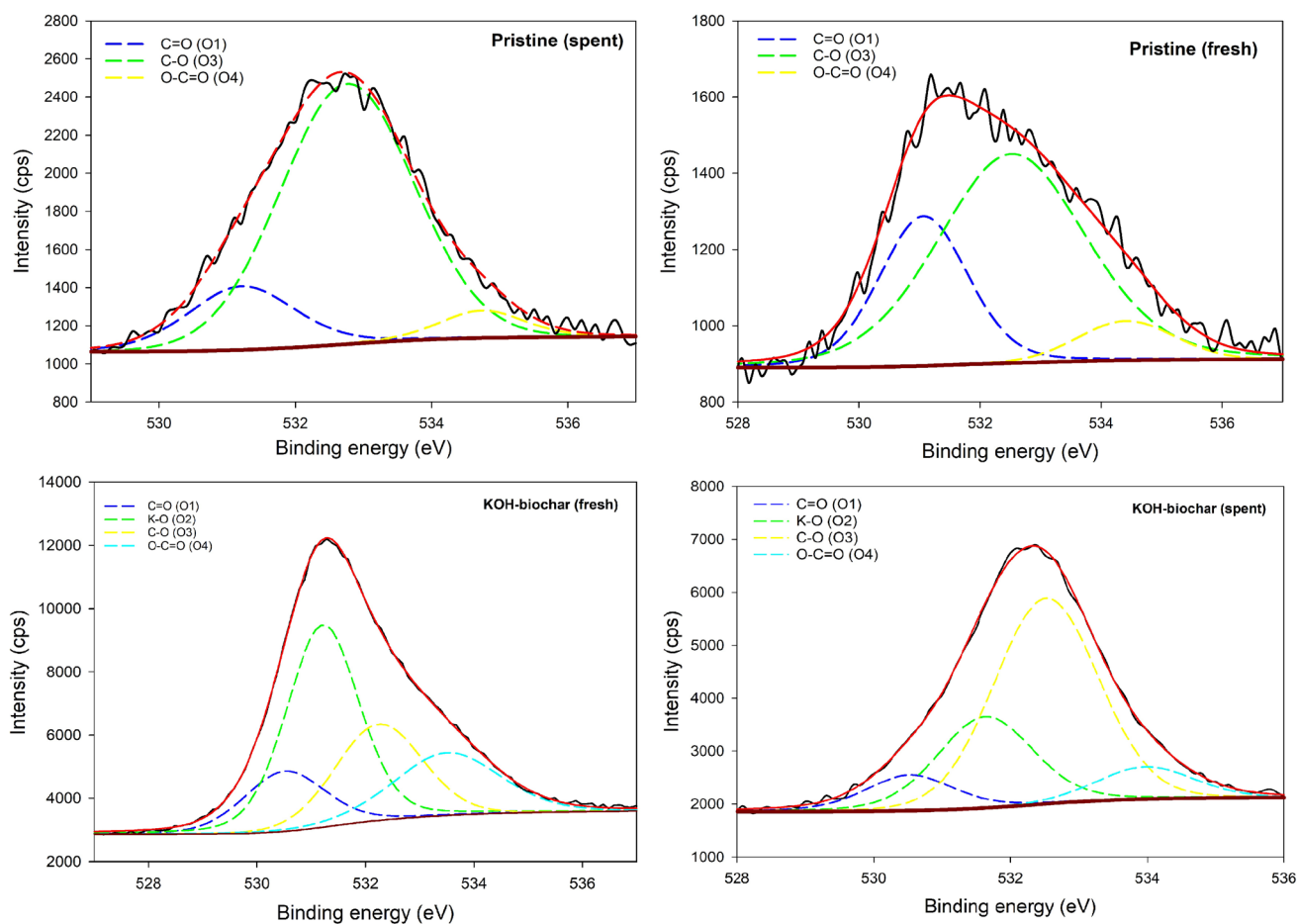
Fig. 5 XPS analysis of O 1s core level for KOH-activated and pristine biochars before (fresh) and after (spent) NO adsorption

532.52 and 533.97 eV were obtained for the KOH-activated biochar after NO adsorption (spent adsorbent). Typically, in the deconvoluted O 1s spectra, the component around 531–532 eV can be assigned to C=O bond and the peak around 531–533 eV may be attributed to K–O bond (Dıaz-Terán et al. 2003). In the spectra of pristine samples (Fig. 5) which were K-free, the peaks around 531 eV were associated with the presence of C=O bonds on the biochar surface, and the ones around 523 and 534 eV were corresponding to C–O and O–C=O bonds, respectively.

Table 2 summarizes the results of deconvolution of O 1s spectra. According to the literature (Tiwari et al. 2018;

Ding and Liu 2020), O1, O2 and O3 in the spectra of KOH-activated biochar have basic nature, while O4 is acidic. The higher proportion of basic groups on the activated biochar surface is hence conductive toward the adsorption of the acidic NO gas. Results in Table 2 indicate that the proportion of C–O increased remarkably after NO adsorption. The proportion of C–O in surface bonds of pristine biochar increased from 64.79% in the fresh sample to 81.28% in the spent adsorbent. While this increment was much more pronounced in case of KOH-activated biochar where the share of C–O in surface bonds remarkably enhanced from 19.59% in fresh adsorbent to 59.82% in the spent sample.

Table 2 Deconvoluted XPS results for O 1s of pristine and KOH-activated biochars before and after NO adsorption

| Binding energy (relative peak areas), eV (%)				
Assignment	C=O	K–O	C–O	O–C=O
KOH-activated biochar (fresh)	530.51 (21.23%)	531.21 (36.82%)	532.24 (19.59%)	533.50 (22.36%)
KOH-activated biochar (spent)	530.52 (7.43%)	531.63 (25.00%)	532.52 (59.82%)	533.97 (7.75%)
Pristine biochar (fresh)	531.06 (27.82%)		532.54 (64.79%)	534.42 (7.40%)
Pristine biochar (spent)	531.24 (14.08%)		532.76 (81.28%)	534.66 (4.64%)

This finding also proves the premise that the adsorbed species on the biochar surface was in the form of C–O–N=O, which could increase the proportion of C–O. This is consistent with the FTIR result whereby a very sharp band around 1380 cm^{-1} was detected, assigning to the vibration of new species formed by the adsorption of NO on biochar surface, which is suggested to be C–O–N=O. This monodentate nitrito species was probably formed from the oxidation of NO on the surface-oxidized groups (Chen et al. 2014). In fact, in the absence of oxygen in the gas phase, NO is only physically adsorbed on the carbon surface; however, the adsorption of NO on biochar surface is rather low (Richter 1990). This is because NO is a supercritical fluid at the ambient condition and thus the extent of its physical adsorption on carbon is low due to the weak adsorbent–adsorbate interaction (Adapa et al. 2006). Yet, the activation of biochar with KOH creates some oxidized groups (C(O)) on biochar surface; they could act as active sites for further oxidation of NO to NO_2, which is more strongly adsorbed than NO (Richter et al. 1990). Indeed, NO is chemisorbed on an oxygen atom of a carbon surface oxide to form a $<C–NO_2>$-complex or NO_2 which is then condensed in micropores:

$$NO(g) + C(O) \rightarrow C–NO_2(ad). \tag{7}$$
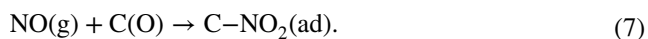
Another possible mechanism for NO_2 formation might be the physical adsorption of NO on vacant active sites of biochar (C_f):

$$NO(g) + C_f \rightarrow C–NO(ad). \tag{8}$$

Then, the NO is oxidized to NO_2 through ion pairing of adsorbed NO and oxygen species following a Langmuir–Hinshelwood-type mechanism. This forms a physically bound NO_2 on the surface and releases an active site for the subsequent NO adsorption (Rubel et al. 1995; Adapa et al. 2006):

$$C–NO(ad) + C(O) \rightarrow C–NO_2(ad) + C_f. \tag{9}$$
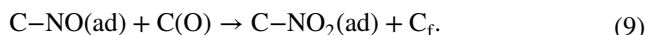
For regeneration of the adsorbent, it might be heated to temperatures above 200 °C where the surface-adsorbed NO_2 can be decomposed to NO and C(O) groups (Guo et al. 2015):

$$C–NO_2 \xrightarrow{T\uparrow} C(O) + NO. \tag{10}$$

Since the generated C(O) groups are unstable, they continue to decompose and create new vacant active sites (Chen et al. 2014):

$$C–C(O) \rightarrow CO + C_f. \tag{11}$$
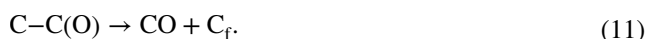
To study the possibility of regeneration of the spent KOH-activated biochar, it was subjected to several cycles of adsorption–desorption, where adsorption was carried out at 30 °C and the desorption was conducted at 220 °C. The NO capture performance of the adsorbent in 12 cycles of temperature swing adsorption–desorption is exhibited in Fig. 6. As observed, the NO uptake capacity dropped from 87.0 to 53.0 mg/g from the first to second cycle and remained almost unchanged thereafter. This indicates that the temperature-induced regeneration was only effective to recover around 61% of the initial adsorption capacity. Most probably, this process could not fully release the chemisorbed NO, and only the physisorbed molecules could be released upon temperature-induced regeneration. This might signify the presence of both reversible and irreversible adsorption sites on the adsorbent. According to the results, it can be assumed that the concentration of irreversible adsorption sites remained almost unaffected after the second cycle where a relatively stable NO uptake capacity could be attained.

Researchers have reported different governing mechanisms for the adsorption of NO on carbon-based materials; for example, Teng and Suuberg (Teng and Suuberg 1993) reported chemisorption for the adsorption of NO on resin char, Rubel et al. (1995) discussed the physisorption mechanism for the capture of NO on activated carbon, Chen et al. (2014) reported both physisorption and chemisorption could control the adsorption of NO on cerium-containing ordered mesoporous carbon, depending on the absence or presence of oxygen in the gas stream and Alcañiz-Monge et al. (2008) reported chemisorption for the adsorption of NO on iron-containing activated carbon fiber. Hence, to understand which adsorption mechanism prevails in this study, kinetic analysis was carried out.
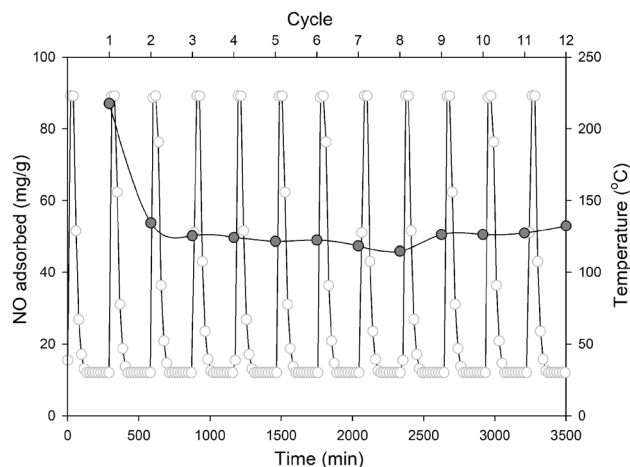

Fig. 6 Cyclic NO uptake performance of KOH-activated biochar; adsorption at 30 °C and desorption at 220 °C

Kinetic studies

To understand the adsorption mechanism of NO adsorption on biochar, several kinetic models including pseudo-first order, pseudo-second order and Elovich were used. The pseudo-first-order model, which is suitable to describe the physisorption and reversible interactions between the gas component and the solid surface, is described by Lagergren rate equation (Chen et al. 2014):

$$\frac{\mathrm{d}q_t}{\mathrm{d}t} = \mathrm{k}_1\left(q_\mathrm{e} - q_t\right) \tag{12}$$

where k_1 is the first-order rate constant (1/min), q_e represents the equilibrium adsorption capacity (mg/g) and q_t is the adsorption capacity at a given time (mg/g). With the boundary conditions of $q_t = 0$ at $t = 0$ and $q_t = q_\mathrm{e}$ at $t = t_\infty$, integrating Eq. (12) gives the exponential form:

$$q_t = q_\mathrm{e}\left(1 - e^{-k_1 t}\right) \tag{13}$$

The pseudo-second-order kinetic model, which is favorable to predict the chemisorption and chemical interactions between the gas and solid surfaces, is expressed as (Kudahi et al. 2017):

$$\frac{\mathrm{d}q_t}{\mathrm{d}t} = k_2\left(q_\mathrm{e} - q_t\right)^2 \tag{14}$$

where k_2 is the second-order rate constant (g/mg.min). This model assumes a linear relationship between the uptake rate and the square of the number of vacant adsorption sites. With similar boundary conditions as those assumed for the previous model, Eq. (14) can be illustrated in the hyperbolic form:

$$q_t = \frac{q_\mathrm{e}^2 k_2 t}{1 + q_\mathrm{e} k_2 t} \tag{15}$$

Another kinetic model to represent the chemisorption of gases on solid surfaces, without the desorption of the product, is Elovich model. The model assumes that the adsorption reaction rate decreases with the increase in the surface coverage and is represented as (Teng and Suuberg 1993):

$$\frac{\mathrm{d}q_t}{\mathrm{d}t} = \alpha \, \exp\left(-\beta q_t\right) \tag{16}$$

where α (mg/g min) is a constant associated with chemisorption rate and β (g/mg) is a constant showing the extent of surface coverage and both constants are temperature-dependent (Inyinbor et al. 2016). When $q_t \rightarrow 0$, the term $\mathrm{d}q_t/\mathrm{d}t$ approaches α; hence, α can be regarded as the initial reaction rate (Juang and Chen 1997; Wu et al. 2009). Assuming the boundary conditions of $q_t = 0$ at $t = 0$ and $q_t = q_t$ at $t = t$ and upon integration, one obtains (Wu et al. 2009):

$$q_t = (1/\beta)\ln\left(1 + \alpha\beta t\right). \tag{17}$$

Assuming $1 << \alpha\beta t$, a simplified Elovich equation will be obtained, which is:

$$q_t = (1/\beta)\ln\left(\alpha\beta t\right). \tag{18}$$

In all these kinetic models, two distinguishable parameters, i.e., kinetic constant and driving force, are found. The kinetic constant accounts for the impact of temperature, and the driving force term shows how far the system is from its equilibrium (Andreoli et al. 2015). In the pseudo-first- and pseudo-second-order kinetic models, the driving force is a power of $(q_\mathrm{e} - q_t)$, while in the Elovich equation the driving force is in the form of an exponential decay factor, wherein the adsorption rate can only be zero at $q_\infty = \infty$ (Andreoli et al. 2015). By theory, this implies that there is no limit to the amount of adsorbed gas, and hence, there is no adsorption plateau.

The experimental data for adsorption of NO over pristine and KOH-activated biochar in the temperature range of 30 to 70 °C were fitted using these three kinetic models. The fitting plot and kinetic parameters of the models are presented in Fig. 7 and Table 3, respectively. Results showed that the experimental adsorption data could be fitted well with all the three models; however, the data could better comply with the Elovich kinetic model. This could be verified by the higher regression coefficients for the Elovich model, especially for KOH-activated biochar, compared to the pseudo-first- and pseudo-second order kinetic models (Table 3). The Elovich model implies a slow chemisorption process that does not reach the adsorption plateau. The experimental data were also indicative of the absence of adsorption plateau where the adsorbent did not saturate after 180 min of adsorption. Teng and Suuberg (1993) also observed that until days after the initiation of the adsorption, the asymptotic NO adsorption on resin char was not reached. This might be due to the stronger diffusion resistance in micropores compared to large and mesopores, which saturate at the early stage of the adsorption, and then, it takes longer time for the gas molecules to fill the micropores of the adsorbent.

The kinetic parameters of Elovich equation are summarized in Table 3. The kinetic parameter α, which can be an estimation of the reaction rate constant, was higher for KOH-activated biochar compared to the pristine biochar at all corresponding temperatures. The value of β was an increasing function of the adsorption temperature. This is consistent with the exothermic nature of the reaction where the adsorption capacity decreased with the increase in the temperature. The experimental data also showed that with the increase in the adsorption temperature from 30 to 40, 50 and 70 °C, the mass uptake reduced from 87.0 to 44.2, 31.7 and 16.8 mg/g, which is attributed to the
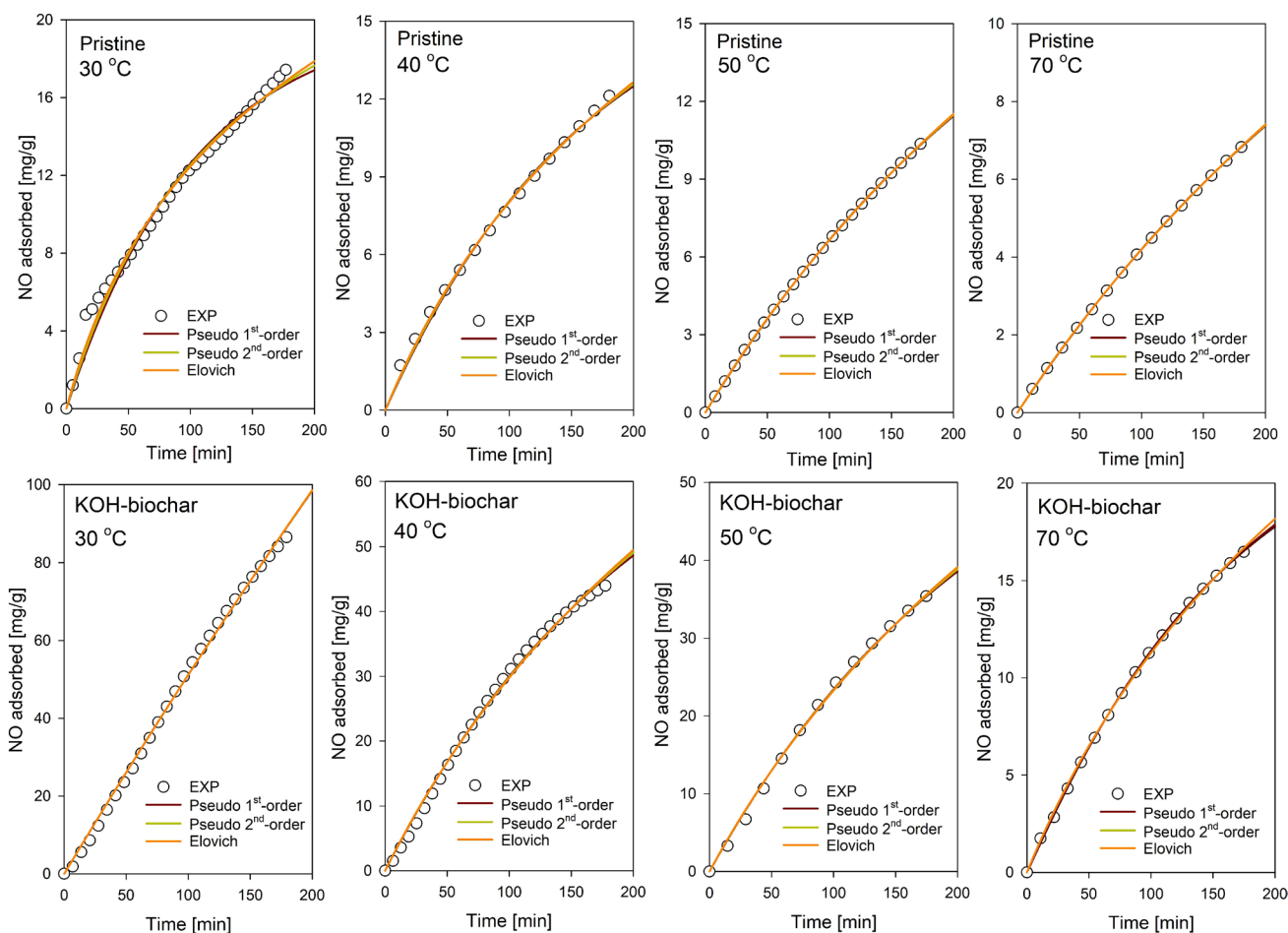
Fig. 7 Plots of pseudo-first-order, pseudo-second-order and Elovich models for adsorption of NO on pristine and KOH-activated biochar

Table 3 Kinetic parameters for the adsorption of NO on pristine and KOH-activated biochar

Kinetic model	Parameter	Pristine biochar				KOH-activated biochar			
		30 °C	40 °C	50 °C	70 °C	30 °C	40 °C	50 °C	70 °C
Pseudo-first-order	$q_{e,exp}$ (mg/g)	17.61	12.12	10.61	6.83	87.02	44.24	36.00	16.85
	k_1 (min^{-1})	0.0140	0.0133	0.0130	0.0119	0.0171	0.0183	0.0171	0.0147
	$q_{e,cal}$ (mg/g)	19.35	13.89	12.78	7.93	139.84	65.95	52.31	20.65
	R^2	0.952	0.963	0.958	0.955	0.8771	0.930	0.916	0.961
Pseudo-second-order	k_2 (g/(mg.min))	0.0012	0.0014	0.0015	0.0022	0.0002	0.0005	0.0005	0.0012
	$q_{e,cal}$ (mg/g)	19.84	13.89	12.94	8.28	121.95	65.79	52.08	23.15
	R^2	0.916	0.963	0.948	0.954	0.913	0.929	0.935	0.941
Elovich	α (mg/(g min))	0.2428	0.1174	0.0803	0.0487	1.623	0.966	0.749	0.374
	β (g/mg)	0.0976	0.0894	0.0548	0.0718	0.0247	0.050	0.062	0.139
	R^2	0.9935	0.9967	0.9999	0.9999	0.9552	0.9842	0.979	0.979

occurrence of the exothermic reversible NO adsorption that reduced the extent of NO adsorption on biochar at higher temperatures.

The temperature-dependent constants α and β in the Elovich equation can be used to determine the activation energy following an Arrhenius-type equation (Andreoli et al. 2015):

$$\ln(\alpha) = C + D/T \tag{19}$$

where C and D are constants. The plot of $\ln \alpha$ vs $1/T$ then will give an estimation of the activation energy. Here, with the increase of the adsorption temperature, the value of α decreased, which implies a negative activation energy. By developing such plots for pristine and KOH-activated biochars (Fig. S4, Supplementary Material), the values of apparent activation energy were obtained from the slope of plots as -26 and -29 kJ/mol for pristine and KOH-activated biochars, respectively. The negative activation energy indicates the decrease of the adsorption rate with increasing temperature; this is consistent with the reversible exothermic nature of the reaction where the adsorption of NO on biochar surface decreased at increased temperatures. The calculated apparent activation energies are low, indicating that the reaction is mainly governed by a physisorption or a weak chemisorption process. Zhang et al. (2008) also reported a low activation energy of -18.5 kJ/mol for NO adsorption on activated carbon. Some studies discussed that the chemisorption of NO on carbon or surface oxygen–carbon complexes at low adsorption temperature (300 K) can be ruled out (Alcañiz-Monge et al. 2008); however, Teng and Suuberg (1993) reported a heat of adsorption of 42 kJ/mol for adsorption of NO on resin char. They discussed that NO could be chemically adsorb on char surface (323–473 K), yet the adsorption process was reversible.

Comparison of the NO uptake capacity of the biomass-based sorbent developed in this study with those available in the literature (Table S1, Supplementary Material) signifies the high potential of this sorbent for the removal of NO from the combustion sources, with near trace concentrations of 300 to 1500 ppm (Rubel et al. 1995).

Conclusion

Low-temperature NO uptake using alkali-modified RSS-derived biochar was investigated. Alkali modification was used to improve the porosity properties and surface chemistry of the pristine biochar. Results indicated that the use of KOH, K_2CO_3, NaOH and Na_2CO_3 as alkali agents improved the NO adsorption capacity of the modified biochar by 3.3 to 3.5 times that of the parent biochar. This remarkable enhancement in NO uptake after alkali activation was mostly attributed to the introduction of oxygenated groups on biochar surface, which play significant role in oxidation of NO to NO_2, increase of the surface basicity which encourages the adsorption of acidic NO gas and improvement of the microporosity of the biochar. Investigations on the activation temperature showed that the increase of the temperature to beyond 700 °C was not effective in improving the NO uptake capacity, yet the effect was very pronounced when the temperature was increased from 600 to 700 °C due to the increase of basic groups on biochar surface. Activation of biochar with KOH at different impregnation ratios indicated that the ratio of 2:1 (KOH: biochar (w/w)) was the best to obtain an NO uptake capacity of 87.0 mg/g. FTIR and XPS analyses of the fresh and spent adsorbents suggested that NO was most probably adsorbed on the biochar surface in the form of C-O-N = O. Kinetic studies were carried out using pseudo-first-order, pseudo-second-order and Elovich models, and the activation energy was determined. The calculated apparent activation energies were low, -26 and -29 kJ/mol for pristine and KOH-activated biochars, respectively, indicating NO adsorption on biochar was mainly governed by a physisorption or a weak chemisorption process. According to the results, the high potential of alkali-activated biochar as a cost-effective and high-capacity sorbent for the removal of NO from flue gas can be highlighted.

Author contributions SIA performed investigation and writing the original draft; PL was involved in visualization, review and editing; MM wrote, reviewed and edited the article; ARM contributed to supervision and funding acquisition.

Declarations

Conflict of interest The authors declare that they have no known competing financial interests or personal relationships that could have appeared to influence the work reported in this paper.

References

Abdulrasheed A, Jalil A, Triwahyono S, Zaini M, Gambo Y, Ibrahim M (2018) Surface modification of activated carbon for adsorption of SO_2 and NO_X: a review of existing and emerging technologies. Renew Sustain Energy Rev 94:1067–1085. https://doi.org/10.1016/j.rser.2018.07.011

Adapa S, Gaur V, Verma N (2006) Catalytic oxidation of NO by activated carbon fiber (ACF). Chem Eng J 116(1):25–37. https://doi.org/10.1016/j.cej.2005.10.007

Ahmad M, Lee SS, Rajapaksha AU, Vithanage M, Zhang M, Cho JS, Lee S-E, Ok YS (2013) Trichloroethylene adsorption by pine needle biochars produced at various pyrolysis temperatures. Bioresour Technol 143:615–622. https://doi.org/10.1016/j.biortech.2013.06.033

Al-Rahbi AS, Williams PT (2016) Production of activated carbons from waste tyres for low temperature NO_x control. Waste Manag 49:188–195. https://doi.org/10.1016/j.wasman.2016.01.030

Alcañiz-Monge J, Bueno-López A, Lillo-Rodenas MÁ, Illán-Gómez MJ (2008) NO adsorption on activated carbon fibers from iron-containing pitch. Microporous Mesoporous Mater

108(1–3):294–302. https://doi.org/10.1016/j.micromeso.2007.04.011

Andreoli E, Cullum L, Barron AR (2015) Carbon dioxide absorption by polyethylenimine-functionalized nanocarbons: a kinetic study. Ind Eng Chem Res 54(3):878–889. https://doi.org/10.1021/ie504277s

Anthonysamy SI, Lahijani P, Mohammadi M, Mohamed AR (2020) Low temperature adsorption of nitric oxide on cerium impregnated biomass-derived biochar. Korean J Chem Eng 37(1):130–140. https://doi.org/10.1007/s11814-019-0405-9

Bakar NA, Othman N, Yunus ZM, Altowayti WAH, Tahir M, Fitriani N, Mohd-Salleh SNA (2021) An insight review of lignocellulosic materials as activated carbon precursor for textile wastewater treatment. Environ Technol Innov. https://doi.org/10.1016/j.eti.2021.101445

Belhachemi M, Jeguirim M, Limousy L, Addoun F (2014) Comparison of NO_2 removal using date pits activated carbon and modified commercialized activated carbon via different preparation methods: effect of porosity and surface chemistry. Chem Eng J 253:121–129. https://doi.org/10.1016/j.cej.2014.05.004

Cao F, Chen J, Ni M, Song H, Xiao G, Wu W, Gao X, Cen K (2014) Adsorption of NO on ordered mesoporous carbon and its improvement by cerium. RSC Adv 4(31):16281–16289. https://doi.org/10.1039/C4RA01409J

Chen J, Cao F, Chen S, Ni M, Gao X, Cen K (2014a) Adsorption kinetics of NO on ordered mesoporous carbon (OMC) and cerium-containing OMC (Ce-OMC). Appl Surf Sci 317:26–34. https://doi.org/10.1016/j.apsusc.2014.08.067

Cheng D, Ngo HH, Guo W, Chang SW, Nguyen DD, Zhang X, Varjani S, Liu Y (2020) Feasibility study on a new pomelo peel derived biochar for tetracycline antibiotics removal in swine wastewater. Sci Total Environ. https://doi.org/10.1016/j.scitotenv.2020.137662

Dehkhoda AM, Ellis N, Gyenge E (2014) Electrosorption on activated biochar: effect of thermo-chemical activation treatment on the electric double layer capacitance. J Appl Electrochem 44(1):141–157. https://doi.org/10.1007/s10800-013-0616-4

Deng W, Tao C, Cobb K, Zhou H, Su Y, Ruan R (2020) Catalytic oxidation of NO at ambient temperature over the chars from pyrolysis of sewage sludge. Chemosphere 251:126429. https://doi.org/10.1016/j.chemosphere.2020.126429

Dıaz-Terán J, Nevskaia D, Fierro J, López-Peinado A, Jerez A (2003) Study of chemical activation process of a lignocellulosic material with KOH by XPS and XRD. Microporous Mesoporous Mater 60(1–3):173–181. https://doi.org/10.1016/S1387-1811(03)00338-X

Ding S, Liu Y (2020) Adsorption of CO_2 from flue gas by novel seaweed-based KOH-activated porous biochars. Fuel 260:116382. https://doi.org/10.1016/j.fuel.2019.116382

Gargiulo V, Gomis-Berenguer A, Giudicianni P, Ania CO, Ragucci R, Alfè M (2018) Assessing the potential of biochars prepared by steam-assisted slow pyrolysis for CO_2 adsorption and separation. Energy Fuels 32(10):10218–10227. https://doi.org/10.1021/acs.energyfuels.8b01058

Ghafari M, Atkinson JD (2016) Catalytic NO oxidation in the presence of moisture using porous polymers and activated carbon. Environ Sci Technol 50(10):5189–5196. https://doi.org/10.1021/acs.est.5b05443

Guo Y, Li Y, Zhu T, Ye M (2015) Investigation of SO_2 and NO adsorption species on activated carbon and the mechanism of NO promotion effect on SO_2. Fuel 143:536–542. https://doi.org/10.1016/j.fuel.2014.11.084

Herath A, Layne CA, Perez F, Hassan EB, Pittman CU Jr, Mlsna TE (2020) KOH-activated high surface area Douglas Fir biochar for adsorbing aqueous Cr (VI), Pb (II) and Cd (II). Chemosphere. https://doi.org/10.1016/j.chemosphere.2020.128409

Inyinbor A, Adekola F, Olatunji GA (2016) Kinetics, isotherms and thermodynamic modeling of liquid phase adsorption of Rhodamine B dye onto Raphia hookerie fruit epicarp. Water Resour Ind 15:14–27. https://doi.org/10.1016/j.wri.2016.06.001

Jjagwe J, Olupot PW, Menya E, Kalibbala HM (2021) Synthesis and application of granular activated carbon from biomass waste materials for water treatment: a review. J Bioresour Bioprod. https://doi.org/10.1016/j.jobab.2021.03.003

Juang R-S, Chen M-L (1997) Application of the Elovich equation to the kinetics of metal sorption with solvent-impregnated resins. Ind Eng Chem Res 36(3):813–820. https://doi.org/10.1021/ie960351f

Kong M, Liu Q, Guo F, Jiang L, Yao L, Ren S, Yang J (2018) Physicochemical properties of pine-derived bio-chars modified by metal oxides and their performance in the removal of NO. J Energy Inst 91(3):467–472. https://doi.org/10.1016/j.joei.2017.01.006

Kudahi SN, Noorpoor AR, Mahmoodi NM (2017) Determination and analysis of CO_2 capture kinetics and mechanisms on the novel graphene-based adsorbents. J CO_2 Util 21:17–29. https://doi.org/10.1016/j.jcou.2017.06.010

Lahijani P, Mohammadi M, Mohamed AR (2019) Catalytic CO_2 gasification of rubber seed shell-derived hydrochar: reactivity and kinetic studies. Environ Sci Pollution Res 26(12):11767–11780. https://doi.org/10.1007/s11356-019-04613-4

Lahijani P, Zainal ZA, Mohammadi M, Mohamed AR (2015) Conversion of the greenhouse gas CO_2 to the fuel gas CO via the Boudouard reaction: a review. Renew Sustain Energy Rev 41:615–632. https://doi.org/10.1016/j.rser.2014.08.034

Lee Y-W, Choi D-K, Park J-W (2002) Performance of fixed-bed KOH impregnated activated carbon adsorber for NO and NO_2 removal in the presence of oxygen. Carbon 40(9):1409–1417. https://doi.org/10.1016/S0008-6223(01)00312-8

Li X, Dong Z, Dou J, Yu J, Tahmasebi A (2016) Catalytic reduction of NO using iron oxide impregnated biomass and lignite char for flue gas treatment. Fuel Process Technol 148:91–98. https://doi.org/10.1016/j.fuproc.2016.02.030

Li Y, Xing B, Ding Y, Han X, Wang S (2020) A critical review of the production and advanced utilization of biochar via selective pyrolysis of lignocellulosic biomass. Bioresour Technol. https://doi.org/10.1016/j.biortech.2020.123614

Nayl A, Elkhashab R, Malah T, Yakout S, El-Khateeb M, Ali M, Ali H (2017) Adsorption studies on the removal of COD and BOD from treated sewage using activated carbon prepared from date palm waste. Environ Sci Pollut Res. https://doi.org/10.1007/s11356-017-9878-4

Nowicki P, Pietrzak R, Wachowska H (2010) Sorption properties of active carbons obtained from walnut shells by chemical and physical activation. Catal Today 150(1–2):107–114. https://doi.org/10.1016/j.cattod.2009.11.009

Reshad AS, Tiwari P, Goud VV (2018) Thermo-chemical conversion of waste rubber seed shell to produce fuel and value-added chemicals. J Energy Inst 91(6):940–950. https://doi.org/10.1016/j.joei.2017.09.002

Richter E (1990) Carbon catalysts for pollution control. Catal Today 7(2):93–112. https://doi.org/10.1016/0920-5861(90)85011-C

Richter E, Schmidt HJ, Schecker HG (1990) Adsorption and catalytic reactions of NO and NH_3 on activated carbon. Chem Eng Technol 13(1):332–340. https://doi.org/10.1002/ceat.270130146

Rubel AM, Stencel JM (1996) Effect of pressure on NOx adsorption by activated carbons. Energy Fuels 10(3):704–708. https://doi.org/10.1021/ef9501861

Rubel A, Stewart M, Stencel J (1995) Activated carbon for control of nitrogen oxide emissions. J Mater Ees 10(3):562–567. https://doi.org/10.1557/JMR.1995.0562

Shen Y, Ge X, Chen M (2016) Catalytic oxidation of nitric oxide (NO) with carbonaceous materials. RSC Adv 6(10):8469–8482. https://doi.org/10.1039/C5RA24148K

Teng H, Suuberg EM (1993) Chemisorption of nitric oxide on char. 1. Reversible nitric oxide sorption. J Phys Chem 97(2):478–483. https://doi.org/10.1021/j100104a033

Thommes M, Kaneko K, Neimark AV, Olivier JP, Rodriguez-Reinoso F, Rouquerol J, Sing KS (2015) Physisorption of gases, with special reference to the evaluation of surface area and pore size distribution (IUPAC Technical Report). Pure Appl Chem 87(9–10):1051–1069. https://doi.org/10.1515/pac-2014-1117

Tiwari D, Bhunia H, Bajpai PK (2018) Adsorption of CO_2 on KOH activated, N-enriched carbon derived from urea formaldehyde resin: kinetics, isotherm and thermodynamic studies. Appl Surf Sci 439:760–771. https://doi.org/10.1016/j.apsusc.2017.12.203

Wu F-C, Tseng R-L, Juang R-S (2009) Characteristics of Elovich equation used for the analysis of adsorption kinetics in dye-chitosan systems. Chem Eng J 150(2–3):366–373. https://doi.org/10.1016/j.cej.2009.01.014

Xiao X, Chen B, Chen Z, Zhu L, Schnoor JL (2018) Insight into multiple and multilevel structures of biochars and their potential environmental applications: a critical review. Environ Sci Technol 52(9):5027–5047. https://doi.org/10.1021/acs.est.7b06487

Yang D-j, Ma X-w, Lv H, Li B, Zhang C-m (2018) NO adsorption and temperature programmed desorption on K_2CO_3 modified activated carbons. J Cent South Univ 25(10):2339–2348. https://doi.org/10.1007/s11771-018-3918-1

Yang J, Zhou J, Tong W, Zhang T, Kong M, Ren S (2019) Low-temperature flue gas denitration with transition metal oxides supported on biomass char. J Energy Inst 92(4):1158–1166. https://doi.org/10.1016/j.joei.2018.06.002

You F-T, Yu G-W, Wang Y, Xing Z-J, Liu X-J, Li J (2017) Study of nitric oxide catalytic oxidation on manganese oxides-loaded activated carbon at low temperature. Appl Surf Sci 413:387–397. https://doi.org/10.1016/j.apsusc.2017.04.044

You F-T, Yu G-W, Xing Z-J, Li J, Xie S-Y, Li C-X, Wang G, Ren H-Y, Wang Y (2019) Enhancement of NO catalytic oxidation on activated carbon at room temperature by nitric acid hydrothermal treatment. Appl Surf Sci 471:633–644. https://doi.org/10.1016/j.apsusc.2018.12.066

Yu JT, Dehkhoda AM, Ellis N (2011) Development of biochar-based catalyst for transesterification of canola oil. Energy Fuels 25(1):337–344. https://doi.org/10.1021/ef100977d

Zhang W, Rabiei S, Bagreev A, Zhuang M, Rasouli F (2008) Study of NO adsorption on activated carbons. Appl Catal B 83(1–2):63–71. https://doi.org/10.1016/j.apcatb.2008.02.003